SAR Marine Applications

Practicals

Martin Gade
Uni Hamburg, Institut für Meereskunde
martin.gade@uni-hamburg.de

Universität Hamburg
DER FORSCHUNG | DER LEHRE | DER BILDUNG

FAKULTÄT
FÜR MATHEMATIK, INFORMATIK
UND NATURWISSENSCHAFTEN

SAR Marine Applications

Friday, 9 Sep, Morning:

1 - History & Basics
- Introduction
- Radar/SAR History
- Basics
- Scatterometer

2 - Wind and Waves
- SAR Wind Fields
- Storms, Tropical Cyclones
- Ocean Surface Waves
- Oceanic Internal Waves
- Marine Surface Films
- Rain

Friday, 9 Sep, Afternoon:

3 - Currents and Objects
- Surface Currents
- Sea Bottom Topography
- Ship Detection
- Oil Pollution Monitoring
- Sea Ice

4 - Practicals
- SNAP Toolbox:
- Georeferencing, Mosaics
- Image Interpretation:
- Wind Fields, Oil Pollution,
- Sea Ice, Objects

Ocean Features on SAR Imagery

Feature	Scale	Derived Measurement	Imaging Mechanism	Wind Speed Range [m s^{-1}]	Characteristics and Considerations
Surface Waves	100 - 600 m wavelength	Wavelength Propagation direction Wave height	Tilt Hydrodynamic Velocity Bunching	3 – 40	Azimuth-traveling waves may be nonlinear without correction. Other limiting factors include wavelength, wave height and fetch.
Internal Waves	0.3 - 3 km wavelength	Wavelength Direction Amplitude Mixed layer depth	Convergence/Divergence Surfactants	2 – 10	Curvilinear packets with multiple waves, decreasing wavelength from front to back. Sensitive to wind conditions, wave crest orientation to platform.
Internal Tides	10 - 20 km	Wavelength Direction	Interaction of centimeter Waves/Currents/Surfactants	3 – 7	
Currents and Fronts	1 - 100 km	Location Shear Strain Velocity	Shear/Convergence Convergence Wind stress Surfactants	3 - 10 3 - 10 3 - 10 3 – 7	Sensitive to wind conditions. Often multiple mechanisms present simultaneously.
Eddies	1 - 200 km diameter	Location and source Diameter Velocity Shear Strain	Shear/Convergence Wind Stress Surfactants	3 - 10 3 - 10 3 – 7	Sensitive to wind conditions. Often multiple mechanisms present simultaneously.
Shallow Water Bathymetry	5 - 50 m depth	Location/change detection Current velocity Depth	Convergence	3 - 12	Sensitive to wind, current properties, depth.

[Jackson & Apel, 2004]

Air-Sea Interactions on SAR Imagery

Feature	Scale	Derived Measurement	Imaging Mechanism	Wind Speed Range [m s^{-1}]	Characteristics and Considerations
Surface Winds	> 1km grid	Wind speed Wind direction	Wind stress Indirectly via windrows, models, or sensors	3 – 25	For mesoscale, coastal variability. Requires good calibration.
Roll Vortices	1 - 5 km wavelength	Boundary Layer: Stratification	Wind stress	3 – 15	Long axis/crests parallel to wind direction.
Gravity Waves	2 - 10 km wavelength	Height Turbulence spectrum Drag coefficient	Wind stress	3 – 15	Long axis/crests perpendicular to wind direction, often associated with topography
Rain Cells	2 - 40 km diameter	Rain rate	Wind stress Rain damping	3 - 15	Appearance sensitive to frequency, rain rate, wind speed.

[Jackson & Apel, 2004]

Surface Films on SAR Imagery

Feature	Scale	Derived Measurement	Imaging Mechanism	Wind Speed Range [m s^{-1}]	Characteristics and Considerations
Biogenic Surfactants	> 100m² area	Areal extent	Convergence	2 – 8	Both forms have signatures similar to low wind, cold thermal water masses, etc.
Mineral Oils	> 100m² area	Areal extent	Seeps Ship discharge Run-off	3 – 15	Wind speed, combination of L- and C-/X-bands may enable discrimination of each form.

[Jackson & Apel, 2004]

Seasat SAR Image

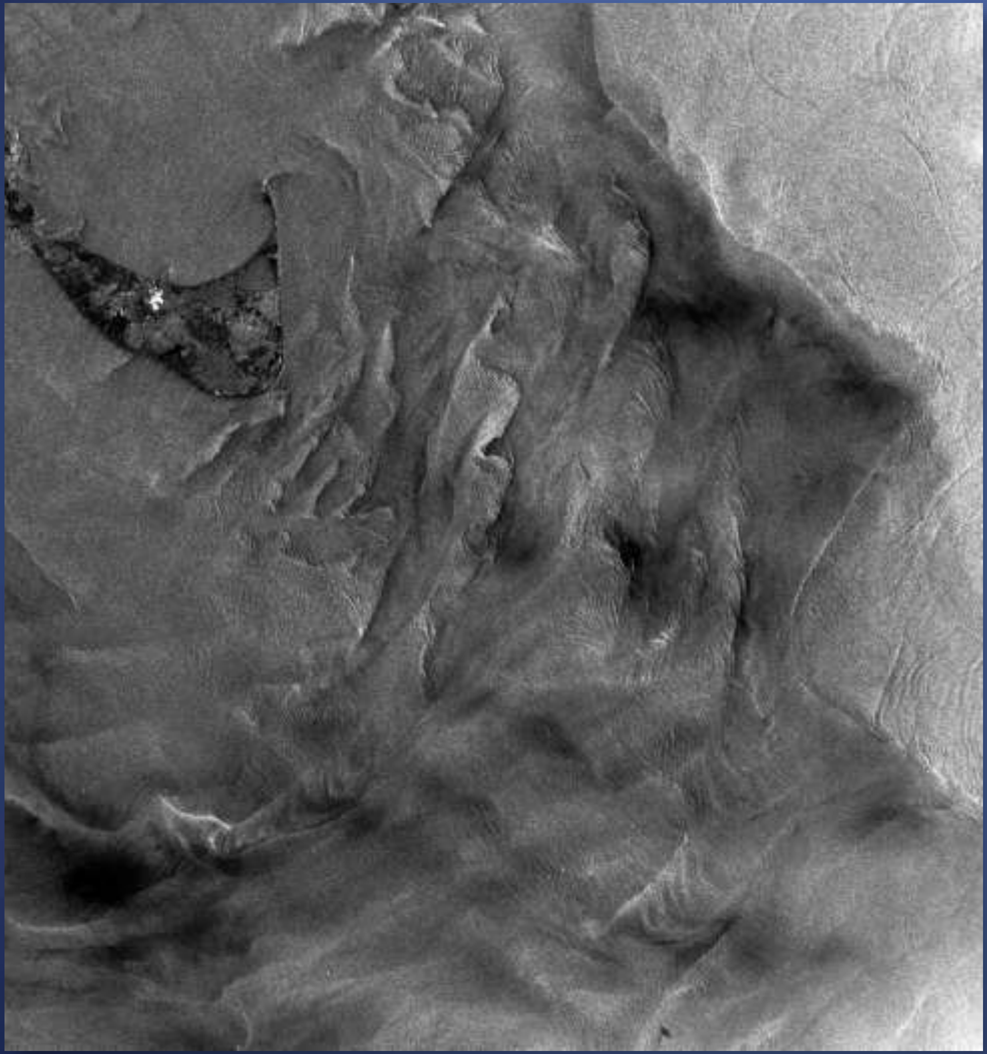

What is shown here?

Seasat SAR Image (L-HH, 80 km × 75 km)
Nantucket Island
(27 August 1978, 12:34 UTC)

Practicals !

Two Sentinel 1A – SAR Images

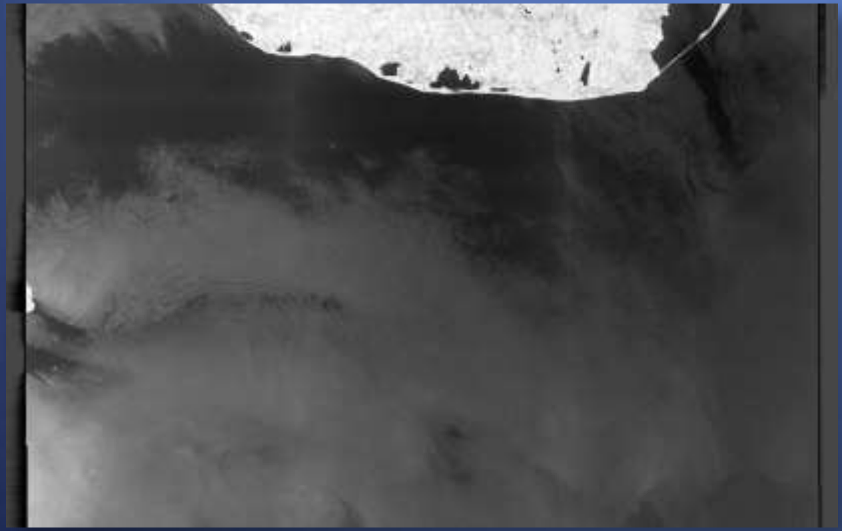

Sentinel 1A SAR Images (C-VV, 259 km × 167 km)
Baltic Proper
(19 August 2016, 16:36 UTC)

Two Sentinel 1A – SAR Images

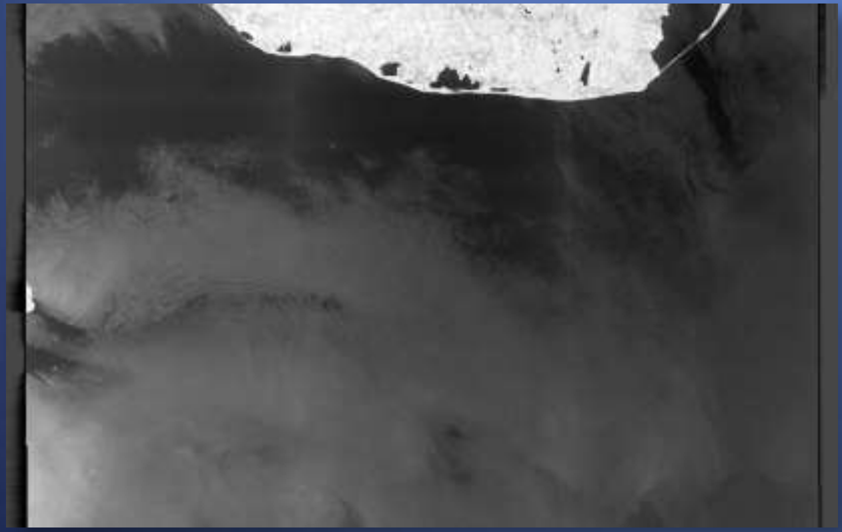

Georeferencing

SNAP:
- Radar
  - Geometric
    - Terrain Correction
      - Range-Doppler TC

Sentinel 1A SAR Images (C-VV, 259 km × 167 km)
Baltic Proper
(19 August 2016, 16:36 UTC)

Two Sentinel 1A – SAR Images

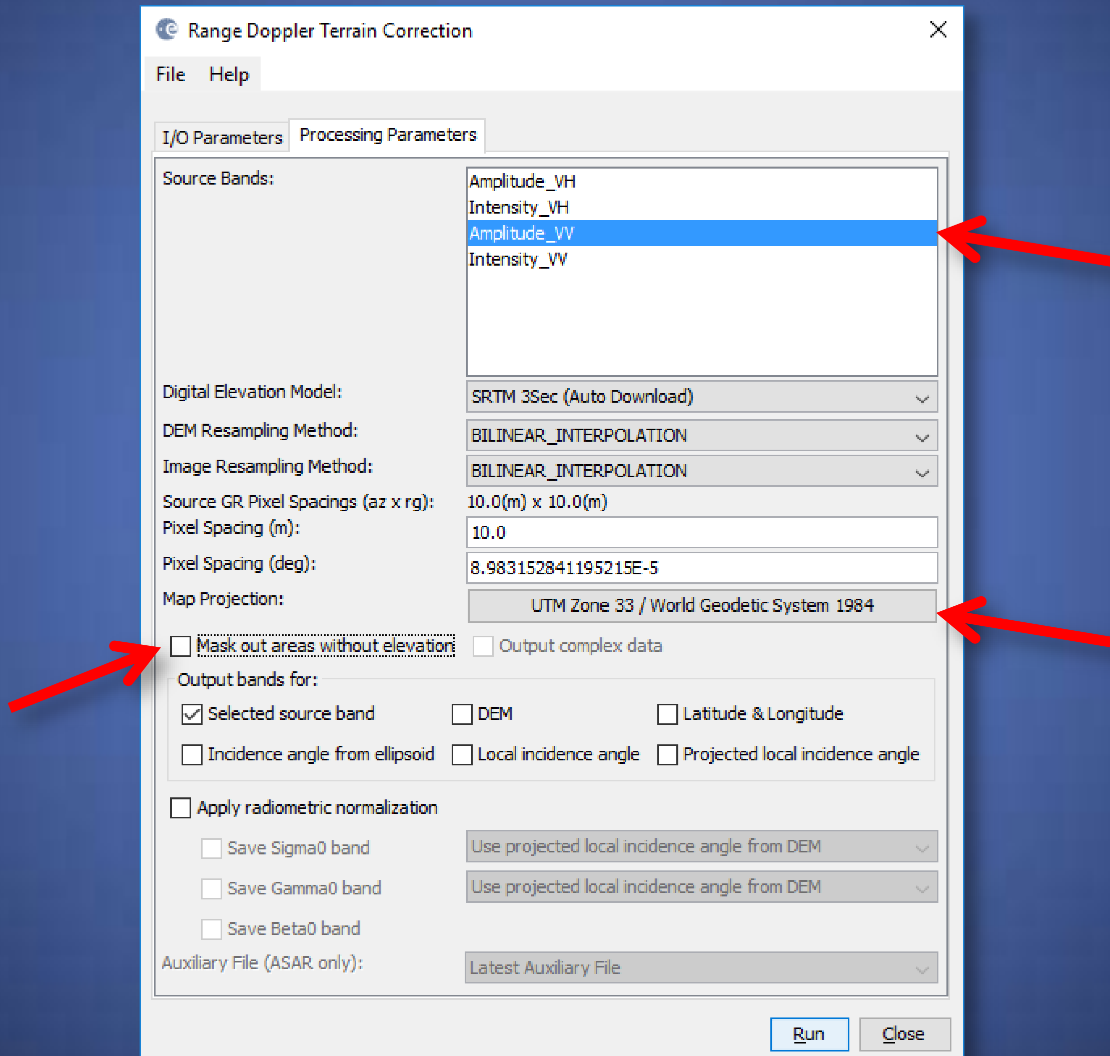

Two Sentinel 1A – SAR Images

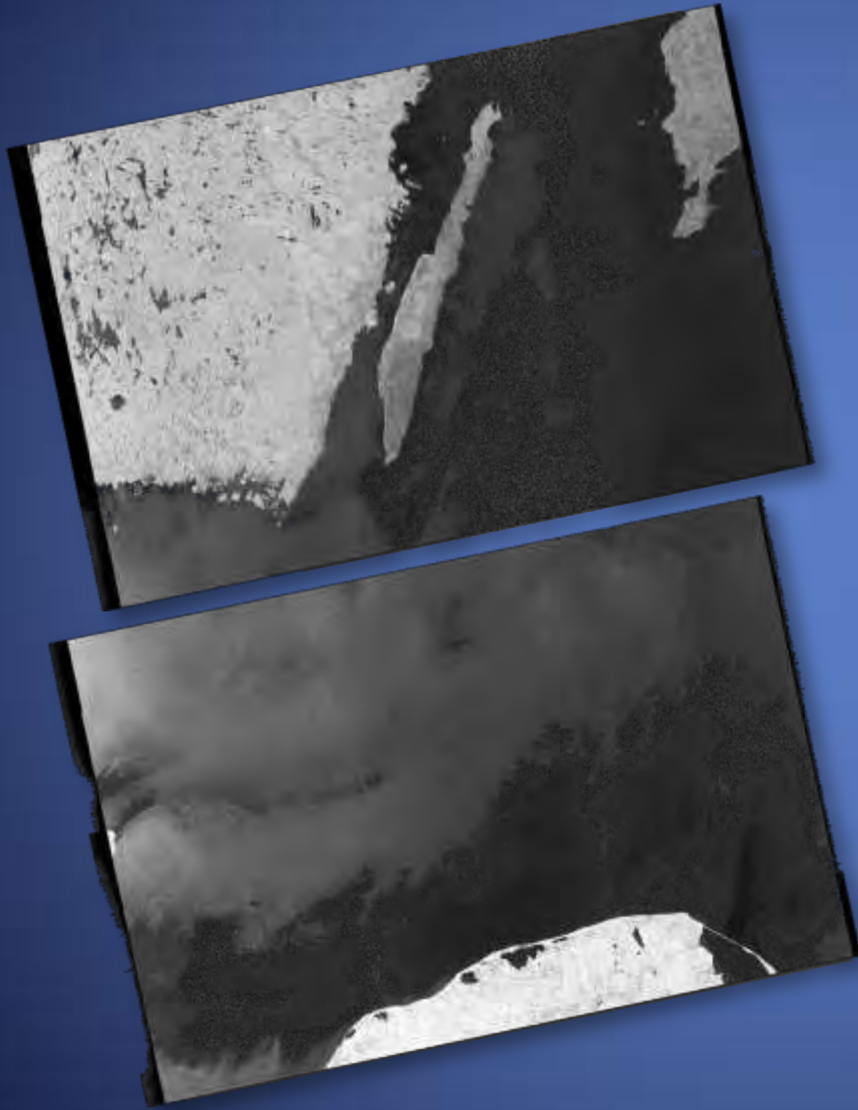

Georeferencing

SNAP:
- Radar
  - Geometric
    - Terrain Correction
      - Range-Doppler TC

Sentinel 1A SAR Images (C-VV, 259 km × 167 km)
Baltic Proper
(19 August 2016, 16:36 UTC)

Two Sentinel 1A – SAR Images

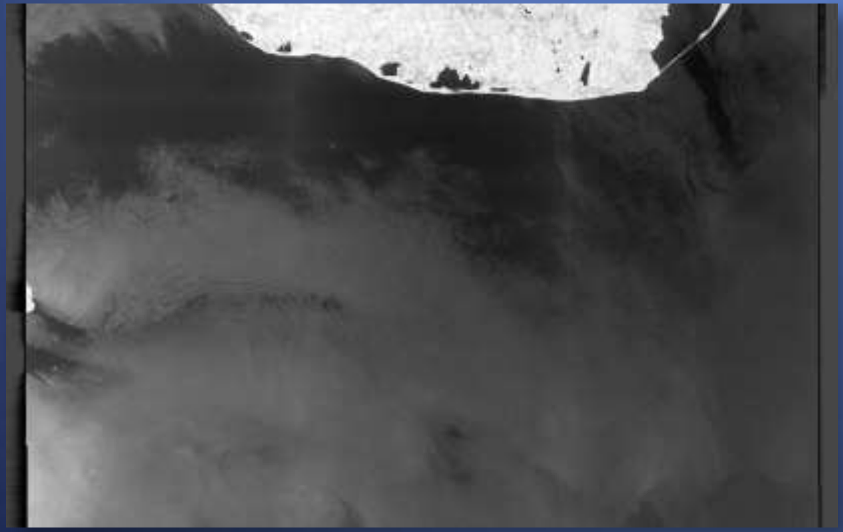

SAR Mosaicking

SNAP:
- Radar
  - Geometric
    - SAR-Mosaic

Sentinel 1A SAR Images (C-VV, 259 km × 167 km)
Baltic Proper
(19 August 2016, 16:36 UTC)

Two Sentinel 1A – SAR Images

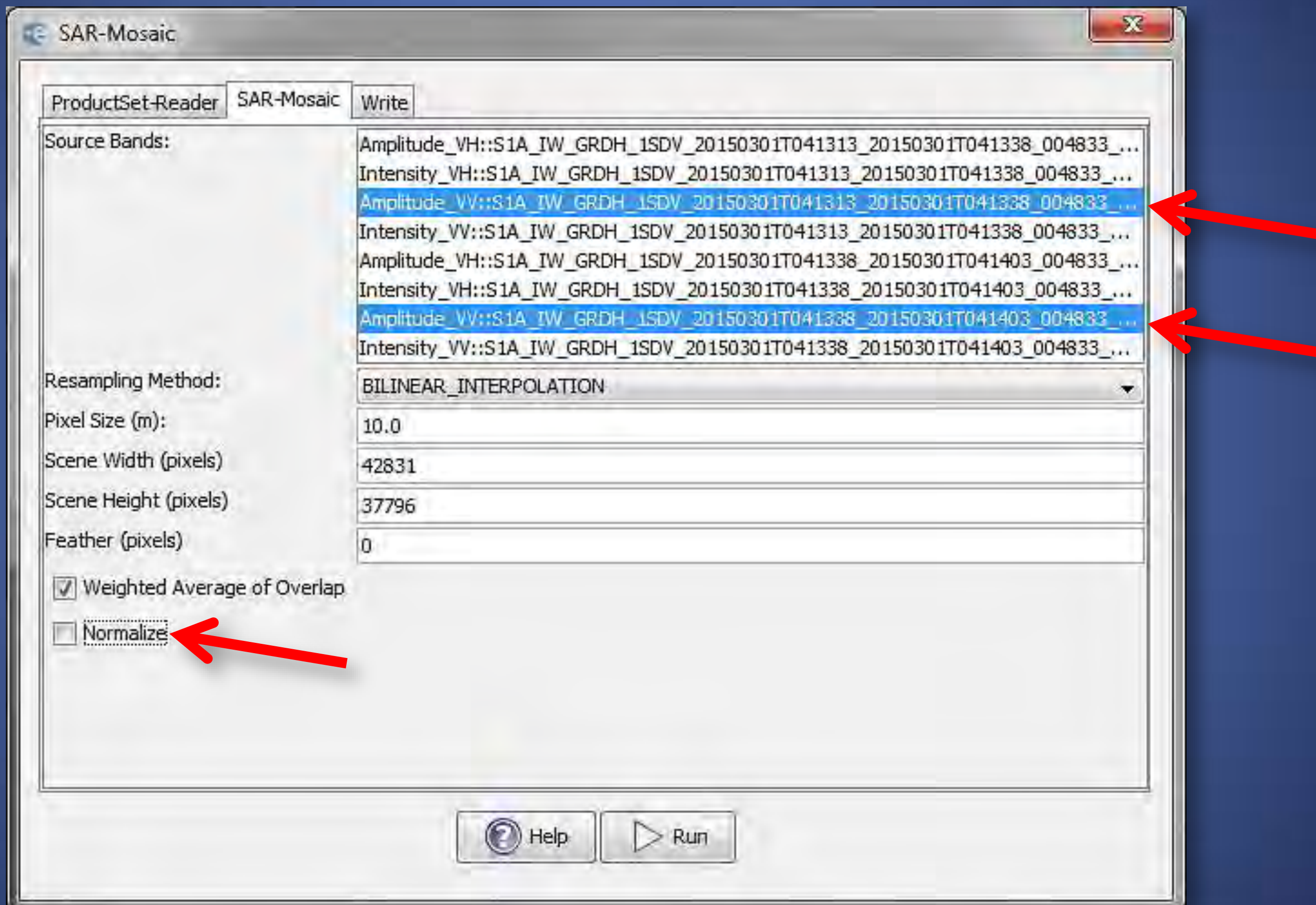

One Sentinel 1A – SAR Mosaic

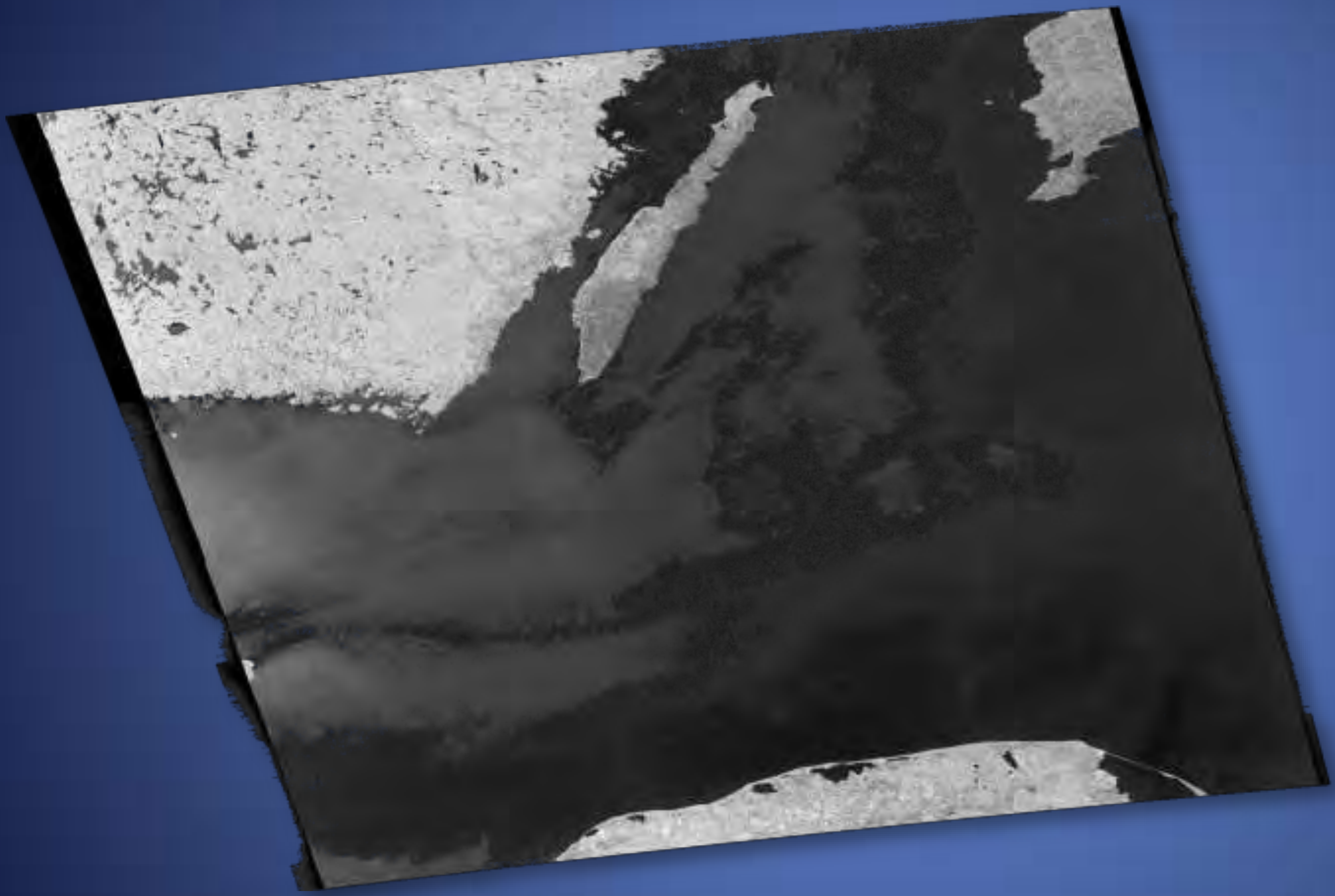

Sentinel 1A SAR Images (C-VV, 259 km × 167 km)
Baltic Proper
(19 August 2016, 16:36 UTC)

One Sentinel 1A – SAR Mosaic

Landmask

SNAP:
- Raster
  - Masks
    - Land/Sea Mask

Sentinel 1A SAR Images (C-VV, 259 km × 167 km)
Baltic Proper
(19 August 2016, 16:36 UTC)

Two Sentinel 1A – SAR Images

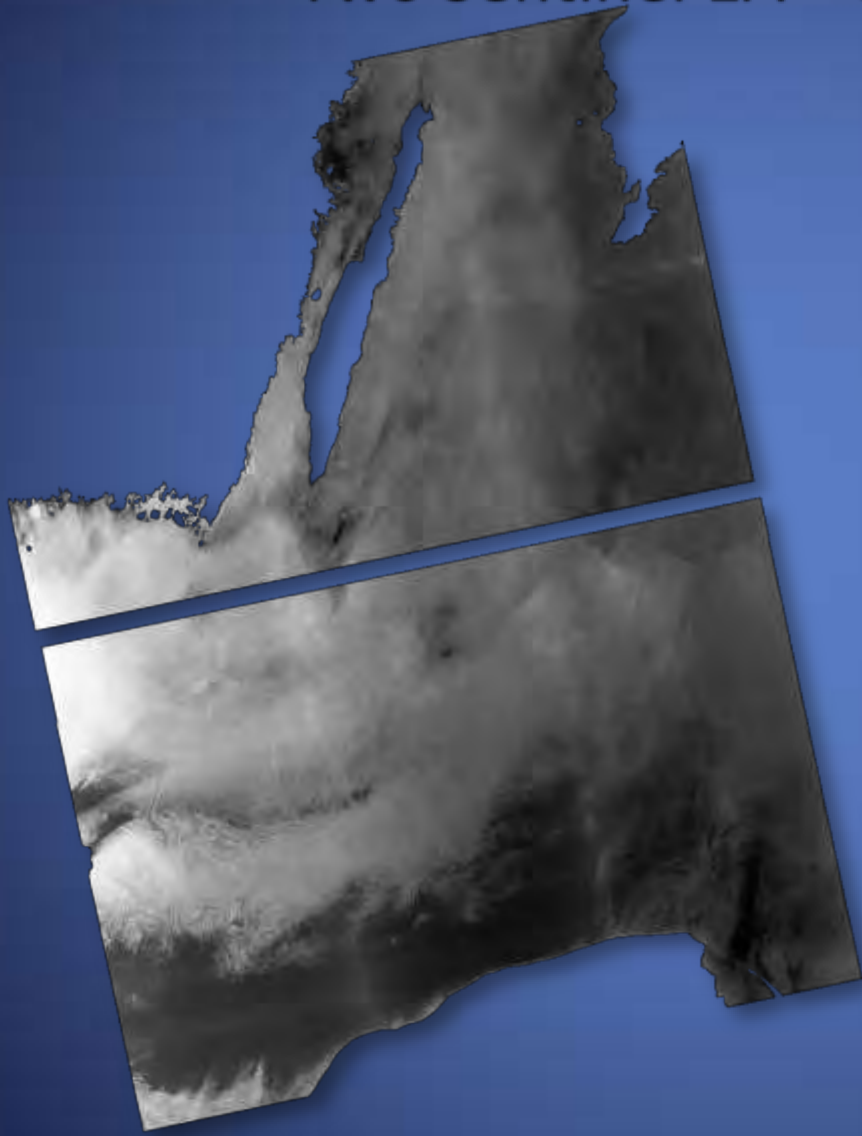

Landmask

SNAP:
- Raster
  - Masks
    - Land/Sea Mask

Different projection!

Sentinel 1A SAR Images (C-VV, 259 km × 167 km)
Baltic Proper
(19 August 2016, 16:36 UTC)

Books: Basics & Theory

Books: Examples and Applications

Some Articles on Basics and Theory

Donelan, M.A., and W.J. Pierson, 1987: Radar scattering and equilibrium ranges in wind-generated waves with application to scatterometry, *J. Geophys. Res., 92*, 4971-5029

Jones, W.L., and L.C. Schroeder, 1978: Radar backscatter from the ocean: dependence on friction velocity, *Boundary Layer Meteor., 13*, 133-149.

Kwoh, D.S., and B.M. Lake, 1985: The nature of microwave backscattering from water waves, in *The Ocean Surface*, Y. Toba & H. Mitsuyasu (Eds), D. Reidel Publishing Company, 249-256.

Liu, W.T., 2002: Progress in scatterometer application, *J. Oceanogr.*, 58, 121-136.

Liu, W.T., X. Xie, and W. Tang, 2010: Scatterometer‘s Unique Capability in Measuring Ocean Surface Stress, in *Oceanography from Space*, V. Barale, J.F.R. Gower, and L. Alberotanza (Eds), Springer, Heidelberg, 93-111.

Phillips. O.M., 1988: Radar returns from the sea surface – Bragg scattering and breaking waves, *J. Phys. Ocean., 18*, 1065-1074.

Valenzuela, G.R., 1978: Theories for the interaction of electromagnetic and oceanic waves – A review, *Boundary Layer Meteor., 13*, 61-85.

Wright, J.W., 1969: A new model for sea clutter, *IEEE Trans. Antennas Propagat., AP-16*, 217-223.

Some Articles on Examples and Applications

Alpers, W., D.B. Ross, and C.L. Rufenach, 1981: On the detectability of ocean surface waves by real and synthetic aperture radar, *J. Geophys. Res.*, **86**, 6481-6498.

Alpers, W., and E. Salusti, 1983: Scylla and Charybdis observed from space, *J. Geophys. Res.*, **88**, 1800-1808.

Alpers, W., and I. Hennings, 1984: A theory of the imaging mechanism of underwater bottom topography by real and synthetic aperture radar, *J. Geophys. Res.*, **89**, 10529-10546.

Brekke, C., and H.A.S. Solberg, 2005: Oil spill detection by satellite remote sensing, *Remote Sens. Environ.*, **95**, 1-13.

Gade, M., W. Alpers, H. Huehnerfuss, H. Masuko, and T. Kobayashi, 1998: The imaging of biogenic and anthropogenic ocean surface films by the multi-frequency/multi-polarization SIR-C/X-SAR, *J. Geophys. Res.*, **103**, 18851-18866.

Gade, M., W. Alpers, C. Melsheimer, and G. Tanck, 2008: Classification of sediments on exposed tidal flats in the German Bight using multi-frequency radar data, *Remote Sens. Environ.*, 112, 1603-1613.

Melsheimer, C., W. Alpers, and M. Gade, 1998: Investigation of multifrequency/ multipolarization radar signatures of rain cells derived from SIR-C/X-SAR data, *J. Geophys. Res.*, **103**, 18867-18884.

Romeiser, R., S. Suchandt, H. Runge, U. Steinbrecher, and S. Grünler, 2010: First analysis of TerraSAR-X along-track InSAR-derived current fields, *IEEE Trans. Geosci. and Remote Sensing*, *48*, 820-829.

Liels paldies!